

# Self-consistency and vertex corrections beyond the *GW* approximation

Arno Schindlmayr\*

Fritz-Haber-Institut der Max-Planck-Gesellschaft, Faradayweg 4–6,  
14195 Berlin-Dahlem, Germany

## Abstract

The good performance of the *GW* approximation for band-structure calculations in solids was long taken as a sign that the sum of self-energy diagrams is converged and that all omitted terms are small. However, with modern computational resources it has now become possible to evaluate self-consistency and vertex corrections explicitly, and the numerical results show that they are, in general, not individually negligible. In this review the available data is examined, and the implications for practical calculations and the theoretical foundation of the *GW* approximation are discussed.

## 1 Introduction

Many-body perturbation theory [1] represents a powerful method for studying the properties of interacting electron systems from first principles that goes beyond the limits of local mean-field approaches. It is based on the Green function, which can be interpreted as a propagator that describes the evolution of an additional electron or hole injected into the system and interacting with its environment via the Coulomb potential. In this way the Green function can be directly related to experimental photoemission spectra in solid state physics, and macroscopic observables like the total energy are obtained through an integral with the respective quantum-mechanical operator. Furthermore, unlike the Kohn-Sham eigenvalues in density-functional theory [2, 3], the resonances of the Green function have a well defined physical meaning as electron addition or removal energies and correspond to the proper quasiparticle band structure. They can be calculated from a modified single-particle Schrödinger equation, in which exchange and correlation effects are rigorously described by the so-called self-energy operator, which takes the form of a nonlocal, energy-dependent potential [4].

A practical way of calculating the self-energy is given by a perturbation expansion in terms of the Coulomb potential and the Green function of the corresponding noninteracting system [1]. This expansion is most conveniently written in the language of Feynman diagrams [5], which may be related to distinct scattering mechanisms. As it is not possible to sum the complete infinite perturbation series, physical intuition can serve to identify the most important contributions. Of course, the selection of diagrams depends on the nature of the problem. In simple metals and semiconductors correlation is predominantly long-range, because electrons interact with their environment through polarization of the surrounding medium and thus

---

\*Correspondence: Dr. Arno Schindlmayr, Fritz-Haber-Institut der Max-Planck-Gesellschaft, Faradayweg 4–6, 14195 Berlin-Dahlem, Germany. E-mail: schindlmayr@fhi-berlin.mpg.de

avoid proximity. This effect is well described by Hedin's *GW* approximation [6], which includes dynamic polarization in the random-phase approximation.

The performance of the *GW* approximation has been discussed in several recent reviews [7, 8]. Most importantly, it corrects the systematic underestimation of semiconductor band gaps in Kohn-Sham density-functional theory, giving very good agreement with experimental data [9, 10]. Another more subtle effect relates to the narrowing of the occupied band width in the alkali metals, which is also described accurately [11, 12]. Because of this success it was long believed that the *GW* approximation indeed captures all relevant self-energy terms for these materials and that the excluded diagrams have negligible weight. However, recent numerical studies that explicitly evaluated self-consistency and vertex corrections, the principal omissions in the *GW* approximation, have cast doubts on this assumption and suggest that the high quantitative accuracy instead stems from a cancellation of errors. A better understanding of these effects would not only strengthen the theoretical foundation of the *GW* approximation, but might also show the way to further systematic improvements. For this reason I review recent progress in this field below and assess the available data.

This paper is organized as follows. In Sec. 2 the *GW* approximation is introduced. Self-consistency and vertex corrections are discussed in Secs. 3 and 4, respectively. Finally, the main points are summarized in Sec. 5. Atomic units are used throughout.

## 2 The *GW* approximation

Many-body perturbation theory is based on the Green function, which is defined as the expectation value of the time-ordered operator product [1]

$$G(1, 2) = -i \langle \Psi | T [\hat{\psi}(1) \hat{\psi}^\dagger(2)] | \Psi \rangle . \quad (1)$$

The short-hand notation  $(1) \equiv (\mathbf{r}_1, \sigma_1, t_1)$  indicates a set of spatial, spin and temporal coordinates,  $|\Psi\rangle$  denotes the normalized ground-state wavefunction in the Heisenberg picture, and  $T$  is Wick's time-ordering operator that rearranges the subsequent symbols in ascending order from right to left. Besides,  $\hat{\psi}^\dagger(2)$  and  $\hat{\psi}(1)$  represent the electron creation and annihilation operator in the Heisenberg picture, respectively. In the absence of a time-dependent external potential, the Green function only depends on the difference  $t_1 - t_2$  and can be mapped to frequency space through a one-dimensional Fourier transform. In the case of noninteracting systems, where the wavefunction is a single Slater determinant, this yields the expression

$$G_0(\mathbf{r}_1, \mathbf{r}_2; \omega) = \sum_{n, \mathbf{k}} \frac{\varphi_{n\mathbf{k}}(\mathbf{r}_1) \varphi_{n\mathbf{k}}^*(\mathbf{r}_2)}{\omega - \epsilon_{n\mathbf{k}} + i \operatorname{sgn}(\epsilon_{n\mathbf{k}} - \mu) \eta} \quad (2)$$

in terms of the solutions

$$\left( -\frac{1}{2} \nabla^2 + V_s(\mathbf{r}) \right) \varphi_{n\mathbf{k}}(\mathbf{r}) = \epsilon_{n\mathbf{k}} \varphi_{n\mathbf{k}}(\mathbf{r}) \quad (3)$$

of the single-particle Schrödinger equation. Here  $\mu$  denotes the chemical potential that separates occupied from unoccupied states and  $\eta$  is a positive infinitesimal. Spin variables have been suppressed, because in the absence of magnetization  $G_0$  is symmetric and diagonal in  $\sigma$ . In the following it is assumed that the single-particle potential  $V_s$  already includes the Hartree potential.

The Green function of an interacting electron system is related to the propagator of the corresponding Hartree system through Dyson's equation [13]

$$G(1, 2) = G_0(1, 2) + \int G_0(1, 3) \Sigma(3, 4) G(4, 2) d(34) . \quad (4)$$

The self-energy operator  $\Sigma$  rigorously describes all exchange and correlation effects. It can be expanded in a perturbation series comprising all connected and topologically distinct diagrams constructed from  $G_0$  and the Coulomb potential  $v$ . As an alternative, Hedin [6] derived a set of exact integral equations that define  $\Sigma$  as a functional of  $G$ . This constitutes a closure relation, which, in combination with Dyson's equation, allows a self-consistent algebraic determination of the Green function. As intermediate quantities, Hedin's equations

$$\Sigma(1, 2) = i \int G(1, 3)W(1^+, 4)\Gamma(3, 2; 4) d(34), \quad (5)$$

$$W(1, 2) = v(1, 2) + \int W(1, 3)P(3, 4)v(4, 2) d(34), \quad (6)$$

$$P(1, 2) = -i \int G(2, 3)G(4, 2)\Gamma(3, 4; 1) d(34), \quad (7)$$

$$\Gamma(1, 2; 3) = \delta(1, 2)\delta(1, 3) + \int \frac{\delta\Sigma(1, 2)}{\delta G(4, 5)}G(4, 6)G(7, 5)\Gamma(6, 7; 3) d(4567) \quad (8)$$

employ the screened Coulomb interaction  $W$ , the polarizability  $P$  and the vertex function  $\Gamma$ . The notation  $(1^+)$  indicates that a positive infinitesimal is added to the time variable.

In principle, this set of equations could be solved by iteration from a suitable starting point, such as  $G_0$ , until self-consistency is reached. However, the occurrence of a functional derivative in Eq. (8) prevents an automatic numerical solution, because it changes the mathematical expression for the integrand in each loop. In practice this means that the starting point must be chosen so close to the expected solution that self-consistency is reached after a very small number of iterations, for which the functional derivative can be evaluated analytically. For solids the Hartree Green function seems a good enough starting point, and solving Hedin's equations with  $\Sigma = 0$  then produces the so-called  $GW$  approximation [6]

$$\Sigma_{GW}(1, 2) = iG(1, 2)W(1^+, 2) \quad (9)$$

after one iteration. The screened interaction enters in the time-dependent Hartree or random-phase approximation, in which the polarization propagator is given by

$$P_{RPA}(1, 2) = -iG(1, 2)G(2, 1). \quad (10)$$

The  $GW$  approximation can be regarded as a generalization of the nonlocal Fock or exchange potential  $\Sigma_x(1, 2) = iG(1, 2)v(1^+, 2)$  with dynamically screened exchange. In addition to Pauli's principle it includes polarization effects and therefore describes correlation between electrons with parallel spin as well as electrons with opposite spin.

To be consistent with the iterative solution of Hedin's equations, the  $GW$  approximation should be evaluated with the Hartree Green function  $G_0$ , although in practice the corresponding Kohn-Sham propagator is typically used [9–12]. A comparison with the exact expression (5) identifies two types of omissions: lack of self-consistency and neglect of vertex corrections. The first group comprises all terms that allow the self-energy to be written in the mathematical form (9) and the polarizability in the form (10) with suitably defined effective propagators. Vertex corrections, on the other hand, stem from an expansion of the vertex function  $\Gamma$ . In this case the topology of the resulting diagrams forbids a reduction to the simple forms above. Some self-energy diagrams are shown in Fig. 1. Arrows represent noninteracting Green functions, the screened interaction is indicated by a wiggly line. The first diagram represents the  $GW$  approximation. The second is a self-consistency term, because it can be absorbed into the first by an appropriate

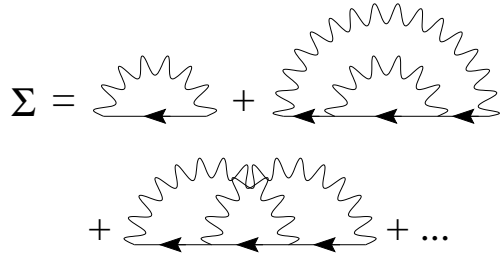


**Figure 1:** Diagrammatic expansion of the self-energy. Arrows represent noninteracting Green functions, the screened interaction is indicated by a wiggly line.

renormalization of the Green function. This is not possible for the third diagram, however, which therefore represents a vertex correction.

Suitable indicators for the assessment of corrections beyond the *GW* approximation are their influence on the band structure, the spectral function and the total energy. The band structure is obtained from

$$E_{n\mathbf{k}} = \epsilon_{n\mathbf{k}} + \langle \varphi_{n\mathbf{k}} | \Sigma(E_{n\mathbf{k}}) | \varphi_{n\mathbf{k}} \rangle . \quad (11)$$

If the single-particle potential  $V_s$  is chosen to include the exchange-correlation potential of density-functional theory, as is typically done in practical calculations, then the self-energy must be replaced by the difference  $\Sigma(E_{n\mathbf{k}}) - V_{\text{xc}}$ . The quasiparticle energies feature as prominent peaks in the spectral function, which is proportional to the imaginary part of the Green function. However, the spectral function also contains other resonances related to many-body excitations. For instance, a quasiparticle excitation may be accompanied by a series of satellites that correspond to the creation or destruction of additional plasmons. Finally, the total energy is given by the Galitskii-Migdal formula [14]

$$E = \frac{1}{\pi} \int_{-\infty}^{\mu} d\omega \int d^3r \lim_{\mathbf{r}' \rightarrow \mathbf{r}} [\omega + h(\mathbf{r})] \text{Im} G(\mathbf{r}, \mathbf{r}'; \omega) , \quad (12)$$

where the one-body Hamiltonian  $h$  contains the kinetic energy operator and the external potential.

### 3 Self-consistency

Although Hedin's equations define the self-energy as a functional of the Green function, which is in turn self-consistently determined by the self-energy through Dyson's equations, most practical calculations simply evaluate the expression (9) using the Green function  $G_0$  of an appropriate noninteracting system. This approach is consistent with Hedin's derivation of the *GW* approximation and generally yields quasiparticle band structures in good agreement with experiments. Nevertheless, from a fundamental point of view this procedure has several shortcomings. First, the use of  $G_0$  in the self-energy introduces an ambiguity, because the result of a *GW* calculation then depends on the choice of the single-particle potential  $V_s$ . Aulbur, Stadele and Gorling [15] recently investigated this effect by comparing a *GW* calculation based on the standard local-density approximation with one starting from an exact exchange and local-density correlation potential. Although the substantial difference in the initial Kohn-Sham band gap is largely levelled out and reduced to about 0.1 eV for most materials considered, in some cases important quantitative discrepancies remain. For instance, for GaAs unreconciled band gaps of 1.16 eV and 1.90 eV are obtained in this way, compared to the experimental value 1.52 eV. Second, without self-consistency the *GW* approximation fails to conserve the particle

number, energy and momentum under time-dependent external perturbations [16]. Even in equilibrium the integral over the spectral function

$$N = \frac{2}{\pi} \int_{-\infty}^{\mu} d\omega \int d^3r \operatorname{Im} G(\mathbf{r}, \mathbf{r}; \omega) \quad (13)$$

does not equal the number of electrons [17], as it should, although the quantitative error is less than 1% for typical semiconductors [18] and the homogeneous electron gas in the range of metallic densities [19]. Furthermore, different methods of calculating the total energy from the Green function are not mutually consistent [20].

Due to the high computational cost, fully self-consistent *GW* implementations, in which the Green function obtained from Dyson's equation (4) is used to update the self-energy until convergence is reached, became possible only a few years ago. The first calculation was probably performed by de Groot, Bobbert and van Haeringen [21] for a quasi-one-dimensional semiconductor, in which the crystal lattice is modelled by a sinusoidal potential. The most important finding is a substantial increase in the band gap, which overestimates the exact Monte-Carlo result and comes close to the Hartree-Fock gap. Furthermore, the weight of the incoherent background in the spectral function is drastically reduced, leading to sharper and more pronounced quasiparticle resonances.

Although the physical characteristics of the model raised doubts concerning its relevance for real materials [7], recent calculations for silicon within a finite-temperature approach have confirmed these findings [22]: while the standard non-self-consistent *GW* approximation widens the indirect band gap from 0.56 eV in the local-density approximation to 1.34 eV, in good agreement with the experimental value 1.17 eV, self-consistency increases the gap to 1.91 eV. The self-consistent *GW* result hence overestimates the experimental band gap by as much as the local-density approximation underestimates it. Besides, self-consistency again leads to an accumulation of spectral weight in the quasiparticle peaks, in disagreement with experiments. The quasiparticle peaks are also narrowed, corresponding to increased lifetimes.

The majority of applications have so far focussed on the homogeneous electron gas, taking advantage of mathematical simplifications due to the spatial isotropy. In addition to fully self-consistent results [19, 20, 23, 24], several studies have reported partially self-consistent calculations in which the Green function  $G$  in Eq. (9) is updated until convergence but the screened Coulomb interaction  $W$  is not [25–27]. In contrast to conventional *GW* calculations, which give an accurate account of the correlation-induced band narrowing, self-consistency causes the occupied band width to increase even above its free-electron value  $k_F^2/2$ , where  $k_F$  denotes the Fermi wave vector. Incidentally, an expansion of the valence band width was also found for silicon [22]. The weight of the quasiparticle peaks is again increased and that of the plasmon satellite reduced accordingly. While the quasiparticle peaks are narrowed, the satellite is broadened and shifted towards the Fermi level. A calculation for potassium shows that the results of the homogeneous electron gas can be fully generalized to metals [22]: the Kohn-Sham band width of 2.21 eV is narrowed to 2.04 eV in the first-order *GW* approximation, improving agreement with the experimental value 1.60 eV. The remaining discrepancy can actually be explained in terms of measurement effects, which shift the apparent peak position of the Fermi level more towards lower binding energies than the state at the bottom of the band and thus give rise to an additional artificial narrowing between 0.2 eV and 0.4 eV [28]. In comparison, the self-consistent *GW* band width is 2.64 eV, much larger even than the Kohn-Sham value.

Taken together, the above results form a consistent picture of the effects of self-consistency, which in a dramatic way reverses the correct trends of conventional *GW* band-structure calculations and destroys the originally good agreement with

experiments. This can be understood as follows. In contrast to  $G_0$ , which refers to a noninteracting system with single-particle excitations only, part of the spectral weight in the interacting Green function  $G$  is transferred to plasmon satellites, which describe collective excitations. The quasiparticle peaks are reduced accordingly. This redistribution of spectral weight in turn implies a smaller dynamic self-energy, i.e., the part  $\Sigma_c = iG(W - v)$  of the self-energy that is due to correlation, in the vicinity of the quasiparticle position. The dynamic self-energy is positive, tending to reduce the band width, and competes with the exchange part  $\Sigma_x$ , which is always negative and increases the band width, e.g., by an amount  $k_F/\pi$  for the homogeneous electron gas in the Hartree-Fock theory [1]. In a self-consistent calculation the smaller dynamic part no longer dominates over the exchange part, which is only marginally reduced, and the band width hence grows rather than narrows [26]. The reduced dynamic self-energy also explains the larger renormalization factors

$$Z_k = \left( 1 - \left. \frac{\partial \text{Re} \Sigma_c(k, \omega)}{\partial \omega} \right|_{\omega=\epsilon_k} \right)^{-1}, \quad (14)$$

which indicate the weight of the quasiparticle resonances, as well as the increase in their lifetime, which is inversely proportional to the imaginary part of  $\Sigma_c$ . The effects described above are further reinforced if the screened interaction is also calculated self-consistently [20]. In this case the sharp plasmon excitations in  $W$  disappear and it no longer has a physical meaning as a response function.

In conclusion, self-consistency is not a good idea for calculating quasiparticle energies without the simultaneous inclusion of vertex corrections. However, an interesting and surprising outcome of the self-consistent  $GW$  calculations for the homogeneous electron gas was the realization that the total energy obtained from the Galitskii-Migdal formula (12) is strikingly close to supposedly exact Monte-Carlo data [20]. It has been speculated [7] that this quite unexpected result is related to the fact that the self-consistent  $GW$  approximation is conserving in the sense of Baym and Kadanoff [16], although relative energy conservation under time-dependent external perturbations does not necessarily imply an accurate total energy on an absolute scale.

Based on the investigation of finite Hubbard clusters, Schindlmayr, Pollehn and Godby [29] note that self-consistency systematically raises the total energy due to an absolute shift of the chemical potential towards higher energies. Likewise, for the homogeneous electron gas the upward transfer of spectral weight from low-lying plasmon satellites to the quasiparticle peak and the increase in the band width, which moves the quasiparticles to lower energies relative to the chemical potential, work in different directions and largely cancel. On the other hand, the chemical potential is shifted upward on an absolute scale, explaining most of the change in the total energy. Although the increase in total energy often leads to better agreement with exact numerical solutions for the finite Hubbard clusters, in some parameter ranges the results become worse. In combination with the unphysical features of the spectral function described above, these observations suggest that the good quantitative agreement with Monte-Carlo data for the homogeneous electron gas may be fortuitous. Recent calculations for the spin-polarized and the two-dimensional electron gas indeed show slightly larger errors [19]. Nevertheless, these results have inspired renewed interest in total-energy calculations within many-body perturbation theory [24, 30, 31].

## 4 Vertex corrections

Vertex corrections introduce additional interaction channels not accounted for in the  $GW$  approximation (9) for the self-energy and the random-phase approxima-

tion (10) for the polarizability. Their effect can be understood by physical interpretation. The random-phase approximation describes dynamic screening within a time-dependent Hartree approach. The screening electrons around a photoemission hole are thus considered independent, exchange and correlation, which enforce spatial separation, are ignored. As a result, the negative charge cloud is too tightly drawn around the central hole and screening at small distances is overestimated, so much, in fact, that the pair distribution function in the random-phase approximation even becomes negative, which is unphysical [32]. Vertex corrections in the polarizability will therefore, in general, reduce the screening and strengthen the interaction. They can also introduce new physical phenomena, such as bound states between the electrons and holes created during a photoemission process. In this case the response function acquires an additional exciton resonance that lies below the plasmon energy. Vertex corrections in the self-energy describe the same exchange and correlation mechanisms between the central photoemission hole and the surrounding particles. The two effects compete and cancel partially: while vertex corrections in the self-energy reduce the probability of finding other holes near the central photoemission hole, vertex corrections in the polarizability simultaneously reduce the screening, thereby increasing the hole density. The change in the quasiparticle energies will hence be small, albeit important. On the other hand, the effect on the satellite spectrum may be drastic, because new types of excitations come into play.

To be consistent, the same vertex function should be used in the self-energy and the polarizability [28,33,34]. However, as the cost of calculating Feynman diagrams grows very rapidly with the topological complexity, nondiagrammatic vertices or plasmon-pole models for the screened interaction have long been the only way to determine higher self-energy terms. Ummels, Bobbert and van Haeringen [35] evaluated the lowest-order vertex correction displayed in Fig. 1 with a plasmon-pole model for silicon and diamond, revising an earlier calculation [36]. While the *GW* approximation increases the direct gap at the  $\Gamma$ -point by 0.78 eV for silicon and 2.12 eV for diamond relative to the local-density approximation, in good agreement with experiments, the vertex diagram yields an additional contribution of  $-0.26$  eV and  $-0.09$  eV, respectively. The results for other high-symmetry points in the Brillouin zone are similar. It hence appears that the vertex corrections can be numerically significant, and the reduction in the band gap tends to cancel the increase due to self-consistency [22]. However, the use of a plasmon-pole model leaves some uncertainties, and it is also known from an early application to the homogeneous electron gas that the lowest-order vertex correction leads to unphysical analytic properties in the self-energy, which can produce regions with a negative density of states [37]. These unphysical features are only cancelled by higher-order terms.

When vertex corrections are taken into account both in the self-energy and the polarizability, their effects tend to cancel to a large degree. For the homogeneous electron gas, Mahan and Sernelius [34] calculated the band width in the range of metallic densities with a static vertex function and obtained essentially the same result as in the *GW* approximation, although there is a strong additional narrowing if vertex corrections are included only in the polarizability. The latter point was actually noted before in relation to the band structure of the alkali metals [11,12]. Likewise, with a vertex function  $\Gamma(1,2;3) = \delta(1,2)f_{xc}(1,3)$ , where  $f_{xc}(1,3) = \delta V_{xc}(1)/\delta n(3)$  denotes the exchange-correlation kernel in the local-density approximation, Del Sole, Reining and Godby [38] found no change in the band gap of silicon, although the absolute position of the bands is shifted by about 0.4 eV. This vertex function is obtained by a consistent first-order solution of Hedin's equations starting from density-functional theory [9] as opposed to Hartree theory, which produces the *GW* approximation. Stronger changes occur if the vertex function is included only in the polarizability and not balanced by

corresponding self-energy diagrams: direct gaps are reduced by up to 0.2 eV and the valence band width decreases by 0.55 eV. Similar conclusions were reached for a finite Hubbard cluster [39].

As expected from the generally good results obtained in the standard *GW* approximation, vertex corrections, if applied in a consistent manner, tend to cancel, inducing subtle but quantitatively small changes in the band structure of solids. Many authors have also reported cancellation between combinations of vertex and self-consistency diagrams for a variety of systems [25, 35, 40]. This observation is reassuring, because it strengthens the theoretical foundation of the *GW* approximation. On the other hand, it leaves the question unanswered how improvements might be achieved. Schindlmayr and Godby [41] proposed a systematic approach based on a continued iterative solution of Hedin's equations. As the *GW* approximation obtained after the first iteration represents a significant and systematic improvement over the zeroth-order Hartree or local-density-approximation, further advances might be achieved by a continuation of this procedure. The implicit integral equation (8) for the vertex function can in fact be solved, and the functional derivative with respect to the full Green function  $G$  is at the same time replaced by a derivative with respect to the known propagator  $G_0$ , which can, in principle, be solved at all levels of iteration. The vertex correction obtained at the end of the second iteration starting from Hartree theory mixes diagrams of different order in the screened interaction. Numerical results for a finite Hubbard cluster show signs of convergence in the excitation energies and suggest that an iterative solution of Hedin's equations may improve the spectrum. However, this approach shares the problem of possible incorrect analytic properties that was earlier noted for the diagrammatic expansion of the self-energy by orders of the screened interaction [37]. Takada [42] proposed a similar approach in which Dyson's equation is solved self-consistently in each iteration, but so far it has only been exploited to derive a solution method for model systems without energy dispersion [43].

Incidentally, more progress has been made with respect to systematic improvements of the satellite spectrum, which from the start is not well rendered in the *GW* approximation. In particular, for the homogeneous electron gas and the alkali metals, the *GW* approximation only produces a single plasmon resonance instead of a sequence of satellites separated from the main peak by multiples of the plasmon frequency. The so-called cumulant expansion remedies this problem by describing the coupling of a quasiparticle to multiple plasmons [44]. It includes the vertex diagram displayed in Fig. 1 as well as corresponding higher-order terms. An application to Na and Al significantly improves the agreement with experimental photoemission spectra, although the relative intensities of the satellites with respect to the quasiparticle peak are still in discrepancy [45]. The quasiparticle position is the same as in the *GW* approximation. In this context it is interesting to note that with vertex corrections, the self-energy is less affected by the deterioration of spectral features, such as the accumulation of spectral weight in the quasiparticle peak and the broadening of plasmon satellites, when applied self-consistently [27]. This is another indicator that the vertex corrections contain the correct physical features. If the exact vertex function is used, then self-consistency must, of course, yield the true spectrum without the mentioned adverse effects.

In a similar way, excitonic effects in the optical absorption spectrum of semiconductors can be accounted for by vertex corrections that describe multiple scattering or binding between electron-hole pairs. This procedure is very computationally demanding, because it requires a calculation of the two-particle Green function. Nevertheless, excitonic vertex corrections have been calculated for several semiconductors and significantly improve the agreement with experimental spectra [46–48].



## 5 Summary

The *GW* approximation is a reliable method for *ab initio* electronic-structure calculations that produces band structure in good agreement with experiments for a wide range of materials. This was originally taken as a sign that higher-order self-energy diagrams are negligible. Statements to this effect indeed frequently appear in the early literature [4]. Only the availability of modern computational resources in recent years has it made possible to explicitly evaluate self-consistency and vertex corrections and test this assumption. The numerical results show that the excluded terms are, in general, not individually small but tend to mutually cancel. The findings of self-consistent calculations are consistent and show a serious deterioration of spectral features compared to the standard *GW* approximation, which can be understood by shifts of spectral weight in the dynamic self-energy. The influence of vertex corrections is naturally less clear-cut, reflecting the large variety of possible vertex functions. However, the case for a mutual cancellation of vertex corrections in the self-energy and the polarizability is well established. Although a general and systematic way of improving quasiparticle energies is still outstanding, physically motivated vertex corrections for better satellite spectra are known.

## Acknowledgments

This work was funded in part by the EU through the NANOPHASE Research Training Network (Contract No. HPRN-CT-2000-00167).

## References

1. Mahan, G.D. 1990, *Many-Particle Physics*, Plenum, New York.
2. Hohenberg, P., and Kohn, W. 1964, *Phys. Rev.* **136**, B864.
3. Kohn, W., and Sham, L.J. 1965, *Phys. Rev.* **140**, A1133.
4. Hedin, L., and Lundqvist, S. 1969, *Solid State Physics*, Vol. 23, H. Ehrenreich, F. Seitz, and D. Turnbull (Eds.), Academic, New York, 1.
5. Feynman, R.P. 1949, *Phys. Rev.* **76**, 749.  
Feynman, R.P. 1949, *Phys. Rev.* **76**, 769.
6. Hedin, L. 1965, *Phys. Rev.* **139**, A796.
7. Aryasetiawan, F., and Gunnarsson, O. 1998, *Rep. Prog. Phys.* **61**, 237.
8. Aulbur, W.G., Jönsson, L., and Wilkins, J.W. 2000, *Solid State Physics*, Vol. 54, H. Ehrenreich and F. Spaepen (Eds.), Academic, San Diego, 1.
9. Hybertsen, M.S., and Louie, S.G. 1985, *Phys. Rev. Lett.* **55**, 1418.  
Hybertsen, M.S., and Louie, S.G. 1986, *Phys. Rev. B* **34**, 5390.
10. Godby, R.W., Schlüter, M., and Sham, L.J. 1986, *Phys. Rev. Lett.* **56**, 2415.  
Godby, R.W., Schlüter, M., and Sham, L.J. 1987, *Phys. Rev. B* **35**, 4170.
11. Northrup, J.E., Hybertsen, M.S., and Louie, S.G. 1987, *Phys. Rev. Lett.* **59**, 819.  
Northrup, J.E., Hybertsen, M.S., and Louie, S.G. 1989, *Phys. Rev. B* **39**, 8198.
12. Surh, M.P., Northrup, J.E., and Louie, S.G. 1988, *Phys. Rev. B* **38**, 5976.
13. Dyson, F.J. 1949, *Phys. Rev.* **75**, 486.  
Dyson, F.J. 1949, *Phys. Rev.* **76**, 1736.
14. Galitskii, V.M., and Migdal, A.B. 1958, *Zh. Eksp. Teor. Fiz.* **34**, 139 [1958, *Sov. Phys. JETP* **7**, 96].
15. Aulbur, W.G., Städele, M., and Görling, A. 2000, *Phys. Rev.* **62**, 7121.
16. Baym, G., and Kadanoff, L.P. 1961, *Phys. Rev.* **124**, 287.  
Baym, G. 1962, *Phys. Rev.* **127**, 1391.
17. Schindlmayr, A. 1997, *Phys. Rev. B* **56**, 3528.

18. Rieger, M.M., and Godby, R.W. 1998, Phys. Rev. B **58**, 1343.
19. García-González, P., and Godby, R.W. 2001, Phys. Rev. B **63**, 075112.
20. Holm, B., and von Barth, U. 1998, Phys. Rev. B **57**, 2108.
21. de Groot, H.J., Bobbert, P.A., and van Haeringen, W. 1995, Phys. Rev. B **52**, 11 000.
22. Schöne, W.-D., and Eguiluz, A.G. 1998, Phys. Rev. Lett. **81**, 1662.
23. Eguiluz, A.G., and Schöne, W.-D. 1998, Mol. Phys. **94**, 87.
24. Holm, B. 1999, Phys. Rev. Lett. **83**, 788.
25. Shirley, E.L. 1996, Phys. Rev. B **54**, 7758.
26. von Barth, U., and Holm, B. 1996, Phys. Rev. B **54**, 8411.  
von Barth, U., and Holm, B. 1997, Phys. Rev. B **55**, 10 120(E).
27. Holm, B., and Aryasetiawan, F. 1997, Phys. Rev. B **56**, 12 825.
28. Shung, K.W.-K., and Mahan, G.D. 1988, Phys. Rev. B **38**, 3856.
29. Schindlmayr, A., Pollehn, T.J., and Godby, R.W. 1998, Phys. Rev. B **58**, 12 684.
30. Holm, B., and Aryasetiawan, F. 2000, Phys. Rev. B **62**, 4858.
31. Sánchez-Friera, P., and Godby, R.W. 2000, Phys. Rev. Lett. **85**, 5611.
32. Pines, D. 1963, *Elementary Excitations in Solids*, W.A. Benjamin, Inc., New York.
33. Ting, C.S., Lee, T.K., and Quinn, J.J. 1975, Phys. Rev. Lett. **34**, 870.
34. Mahan, G.D., and Sernelius, B.E. 1989, Phys. Rev. Lett. **62**, 2718.
35. Ummels, R.T.M., Bobbert, P.A., and van Haeringen, W. 1998, Phys. Rev. B **57**, 11 962.
36. Bobbert, P.A., and van Haeringen, W. 1994, Phys. Rev. B **49**, 10 326.
37. Minnhagen, P. 1974, J. Phys. C **7**, 3013.  
Minnhagen, P. 1975, J. Phys. C **8**, 1535.
38. Del Sole, R., Reining, L., and Godby, R.W. 1994, Phys. Rev. B **49**, 8024.
39. Verdozzi, C., Godby, R.W., and Holloway, S. 1994, Phys. Rev. Lett. **74**, 2327.
40. de Groot, H.J., Ummels, R.T.M., Bobbert, P.A., and van Haeringen W. 1996, Phys. Rev. B **54**, 2374.
41. Schindlmayr, A., and Godby R.W. 1998, Phys. Rev. Lett. **80**, 1702.
42. Takada, Y. 1995, Phys. Rev. B **52**, 12 708.
43. Takada, Y., and Higuchi, T. 1995, Phys. Rev. B **52**, 12 720.
44. Langreth, D.C. 1970, Phys. Rev. B **1**, 471.
45. Aryasetiawan, F., Hedin, L., and Karlsson K. 1996, Phys. Rev. Lett. **77**, 2268.
46. Albrecht, S., Onida, G., and Reining, L. 1997, Phys. Rev. B **55**, 10 278.  
Albrecht, S., Reining, L., Del Sole, R., and Onida, G. 1998, Phys. Rev. Lett. **80**, 4510.
47. Benedict, L.X., Shirley, E.L., and Bohn, R.B. 1998, Phys. Rev. B **57**, R9385.  
Benedict, L.X., Shirley, E.L., and Bohn, R.B. 1998, Phys. Rev. Lett. **80**, 4514.
48. Rohlfing, M., and Louie, S.G. 1998, Phys. Rev. Lett. **81**, 2312.